Article

Feature Extraction with Discrete Non-Separable Shearlet Transform and Its Application to Surface Inspection of Continuous Casting Slabs

Xiaoming Liu [1] , **Ke Xu** [2,*] , **Peng Zhou** [1] **and Huajie Liu** [2]

1 National Engineering Research Center for Advanced Rolling Technology, University of Science and Technology Beijing, Beijing 100083, China; jklxm333@e-mail.com (X.L.); zhoupeng@nercar.ustb.edu.cn (P.Z.)
2 Collaborative Innovation Center of Steel Technology, University of Science and Technology Beijing, Beijing 100083, China; lhjk2s@163.com
* Correspondence: xuke@ustb.edu.cn; Tel.: +86-10-62332159

check for updates

Featured Application: First, the surface defect inspection characteristics of continuous casting slab is that the slab moves slowly on the production line, so the feature extraction method does not need too fast a calculation speed. Second, the inspection difficulties of continuous casting slabs are the defect with complex backgrounds, so some common feature extraction methods cannot meet these needs. DNST (discrete non-separable shearlet transform) is a new multiresolution analysis method with moderate computing speed. It can extract images information from multiple scales and directions. Therefore, this paper proposed a DNST-GLCM-KSR (discrete non-separable shearlet transform-gray-level co-occurrence matrix-kernel spectral regression) feature extraction method. The method is suitable for surface defects inspection with complex background and moderate running speed of production line.

Abstract: A new feature extraction technique called DNST-GLCM-KSR (discrete non-separable shearlet transform-gray-level co-occurrence matrix-kernel spectral regression) is presented according to the direction and texture information of surface defects of continuous casting slabs with complex backgrounds. The discrete non-separable shearlet transform (DNST) is a new multi-scale geometric analysis method that provides excellent localization properties and directional selectivity. The gray-level co-occurrence matrix (GLCM) is a texture feature extraction technology. We combine DNST features with GLCM features to characterize defects of the continuous casting slabs. Since the combination feature is high-dimensional and redundant, kernel spectral regression (KSR) algorithm was used to remove redundancy. The low-dimension features obtained and labels data were inputted to a support vector machine (SVM) for classification. The samples collected from the continuous casting slab industrial production line—including cracks, scales, lighting variation, and slag marks—and the proposed scheme were tested. The test results show that the scheme can improve the classification accuracy to 96.37%, which provides a new approach for surface defect recognition of continuous casting slabs.

Keywords: continuous casting slabs; surface defect classification; discrete non-separable shearlet transform; gray-level co-occurrence matrix; kernel spectral regression

1. Introduction

At present, machine vision–based surface inspection technology has been widely used in the detection and identification of surface defects of various industrial products due to its non-contact and real-time detection properties [1]. The machine vision–based detection method is to collect the

image of the industrial product under the irradiation of the high-intensity light source and use the image processing and pattern recognition algorithm to analyze the surface image [2]. For different industrial products, one need consider defect image features of the products themselves and then adopt appropriate recognition methods.

In the production process of continuous casting slabs, defects often occur due to various factors like raw material, preprocessing technologies, etc. The defects will have a negative impact on the next rolling process, and severe defects will even lead to the scrapping of entire slabs [3,4]. The defect feature extraction method plays an important role in defect inspection, which is one of the hotspots in the research on surface defect recognition algorithms. The most important characteristic of surface defects of continuous casting slab are complex backgrounds, which make recognition difficult.

At present, research is more active on strip steel products with a simple background image [5–7]. However, the defect recognition of continuous casting slabs with complex backgrounds has received comparatively little attention. Wei SY et al. [3] extracted the shape feature values of the image to classify and recognition defects. Yun [8] proposed a surface defect recognition algorithm based on Gabor wavelet that can detect the fine cracks and angular cracks on the surface of the slabs by minimizing the cost function of the energy separation criterion for the defect area and the defect-free area. Pan E [9] proposed an engineering-driven rule-based detection (ERD) method according to the mechanism of deep longitudinal crack and transverse crack on slabs. Xu K et al. [10] used non-sampled wavelet to decompose the surface image by calculating the scale co-occurrence matrix and grayscale co-occurrence matrix, and used AdaBoosting classifier to identify cracks from water marks, slag marks, scales, and vibration marks. Subsequently, the author proposed combining the discrete shearlet transform (DST) and kernel local preservation projection (KLPP) algorithm to extract surface defect features [2]. Y. Ai utilized the combination of Contourlet transform and kernel local preservation projection (KLPP) algorithm to extract the defect features [1], then Xu K [11] improved the above method by introducing a texture feature. Si Yang [12] improved the local binary pattern and proposed a multi-block local binary pattern (MB-LBP) feature extraction method.

Of the above mentioned methods, the wavelet-based feature extraction (for example, references [1,2,8,10,11]) is the more effective and more studied technology. Although these methods have achieved some results, the recognition accuracy of surface defects of continuous casting slabs needs to be further improved with the increasingly strict quality requirements of users.

Discrete nonseparable shearlet transform (DNST) [13,14] is a new kind of wavelet-based method. It is a compactly supported shearlet transform with excellent localization properties in the spatial domain and excellent directional selectivity. DNST has been successfully introduced in the fields of compressed sensing magnetic resonance imaging [15,16]. According to defect images of continuous casting slabs with the scale and directionality traits, DNST was introduced into the surface defect feature extraction of continuous casting slabs. The gray-level co-occurrence matrix (GLCM) is an effective texture feature extraction method that can reflect the comprehensive information of the image gray in direction, adjacent pixel interval, and gray level variation [17]. Some defects images of continuous casting slabs also have texture traits, thus we consider introducing GLCM into the feature extraction of continuous casting slabs. Since the features extracted by DNST and GLCM are redundant, we use kernel spectral regression (KSR) [18,19] technology to remove redundant features. KSR is a kind of manifold learning dimensionality reduction technology, and it casts the problem of learning an embedding function into a regression framework that facilitates efficient computations. The proposed feature extraction approach is named discrete nonseparable shearlet transform gray-level co-occurrence matrix kernel spectral regression (DNST-GLCM-KSR), which combines multi-scale and multi-directional features of DNST with texture features of GLCM and uses KSR to remove redundant features. The DNST-GLCM-KSR approach can improve the defect recognition accuracy of continuous casting slabs and achieved better performance than traditional methods.

The novelty of our work lies in introducing DNST into the surface defect recognition of continuous casting slabs with the complex backgrounds, fusing GLCM texture features, and using a suitable

dimensionality reduction algorithm KSR, which makes defect recognition easier and more effective. The rest of this paper is organized as follows. In Section 2, the surface defects information of continuous casting slabs is depicted. Section 3 introduces the basic principles of the DNST-GLCM-KSR feature extraction approach. The surface defect recognition algorithm is presented in Section 4. Section 5 describes the experimental results and discussions, followed by conclusions in Section 6.

2. The Characteristics of Defect Images

The surface temperature of continuous casting slabs is very high during the production process. The temperature can reach about 800~900 °C, which results in the surface being oxidized and forming a large number of various shapes scales [1]. The scales seriously interfere with the detection and recognition of defects. At the same time, due to insufficient illumination in the production site and the rough surface of continuous casting slabs, the slab surface appears uneven. Also, in the continuous casting slab production process, the quality of surface images collected is decreased due to the splash of cooling water, rolling mill vibrations, and other factors. Figure 1 shows several common surface images of continuous casting slabs, including cracks, scales, lighting variations, and slag marks. The cracks are true defect, while the scales, lighting variations, and slag marks are the interference factors that may lead to misclassification. The interference factors are labeled as false defects and also as a type of recognition object. The main task of continuous casting slabs is to recognize crack defects in the complicated background and interference factors.
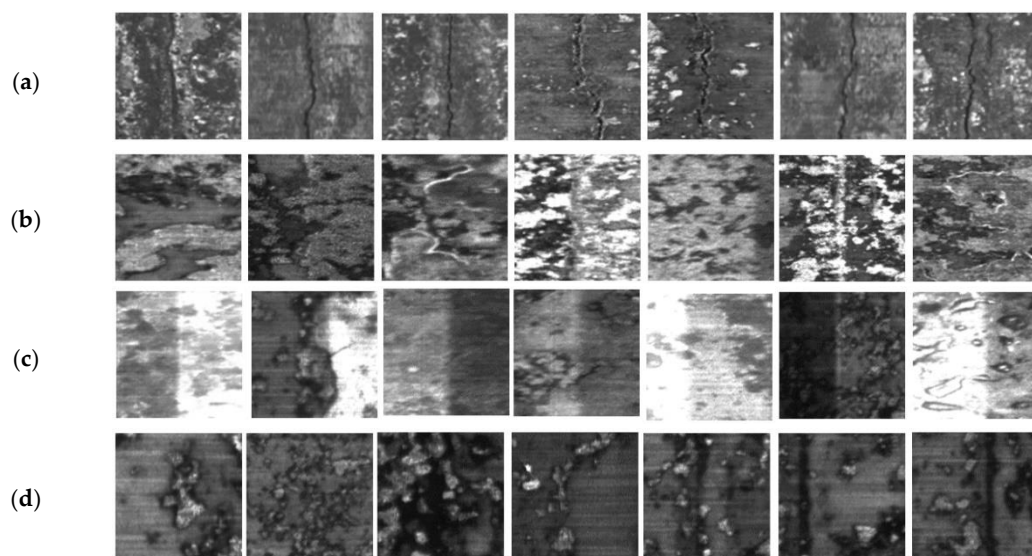

Figure 1. Surface images of continuous casting slabs. (**a**) Cracks; (**b**) Scales; (**c**) Lighting variations; (**d**) Slag marks.

Figure 1a is longitudinal crack defect sample, abbreviated as cracks. The cracks are mainly along the longitudinal distribution of the slabs, the shape is curved, and the length ranges from a few centimeters to dozens of centimeters. The cracks usually have a certain depth, which shows a different grayscale value than the surrounding pixels in the intense light irradiation. The occurrence of cracks is mostly related to the high-temperature steel and various mechanical behaviors in the solidification process. A crack is a very serious defect.

Figure 1b is a scales sample. The shape of scales is uncertain and varies greatly. Sometimes, some of the scales are warped, but most scales are attached to the surface of the slabs and show texture features. Due to the scales covering the surface of the slabs, some fine crack defects are hard to identify.

Figure 1c is the lighting variations. The bright and dark areas are caused by the irradiation of multiple light sources or changes in illumination intensity. The boundaries of the bright and dark areas

show straight line shapes, and the gray values on both sides are noticeably different. Therefore, these boundaries are sometimes misclassified as cracks.

Figure 1d is the slag marks. They are mainly formed by the residual slag. Slag marks are also distributed along the longitudinal direction of the slabs with a certain width, and their gray values are lower than that of the surrounding pixels. These images are easily misclassified as crack defects.

3. Basic Principles of the Proposed Method

The feature extraction method is the core of the defect recognition algorithm. The quality of feature extraction directly affects the results of defect recognition. The proposed feature extraction scheme DNST-GLCM-KSR in this paper utilizes three technologies, including DNST, GLCM, and KSR, which are described in detail as follows.

3.1. Discrete Nonseparable Shearlet Transform

The wavelet analysis method has been applied in many fields due to its advantages of multi-scale decomposition and fast computation speed. However, the drawback of the wavelet is that the direction decomposition is insufficient. It can only decompose the horizontal, vertical, and diagonal directions. In order to compensate for the deficiency of directional decomposition, the multi-scale geometric analysis (MGA) method was proposed. Typical multi-scale geometric analysis methods include Ridgelet transform [20], Curvelet transform [21], Contourlet transform [22], Shearlet transform [23], and Bandelet transform [24]. The most widely used ones are Contourlet transform and Shearlet transform, while the other methods are limited by their slow computational speed. The advantage of Contourlet is fast computational speed, but its direction representation is limited. The computational speed of Shearlet transform is slower than that of Contourlet, but the direction representation is more flexible. The continuous casting slabs run very slowly on the track, with a speed less than 1 m/s, so the computational speed of the defect recognition algorithm is not required to be fast. The discrete nonseparable shearlet transform (DNSTS) [13,14] is a new kind of shearlet transform.

W.Q. Lim [13] proposed discrete nonseparable shearlet transform (DNST) based on the discrete frame. DNST is constructed from a 2D nonseparable fan filter (improved directional selectivity) and a separable compactly supported shearlet generator (excellent localization properties). It is a direction representation system that extends the wavelet frame. DNST exhibits the same advantages wavelet, namely a unified treatment of the continuum and digital situation.

Two-dimensional discrete shearlet transform is usually obtained using a cone adapted discrete shearlet system defined by scaling functions ϕ_m and shearlet functions $\psi_{j,k,m}$, $\widetilde{\psi}_{j,k,m}$ (by swapping the order of two variables of $\psi_{j,k,m}$).

$$\left\{\phi_m : m \in \mathbb{Z}^2\right\} \cup \left\{\psi_{j,k,m}, \widetilde{\psi}_{j,k,m} : j \in Z, j \geq 0, |k| \leq 2^{\frac{j}{2}}; m \in \mathbb{Z}^2\right\} \tag{1}$$

where *j* is scaling parameter, *m* is translation parameter, and *k* is shear (direction) parameter.

Non-separable generator ψ^{non} is defined as follows:

$$\hat{\psi}^{non}(\xi) = P(\xi_1/2, \xi_2)\hat{\psi}(\xi) \tag{2}$$

where the trigonometric polynomial *P* is a 2D fan filter, which can improve directional selectivity in the frequency domain at each scale. ψ is the 2D separable shearlet generator. which can provide excellent localization properties. $\hat{\psi}$ is the Fourier transform of ψ. The nonseparable shearlets $\psi^{non}_{j,k,m}(x)$ generated by ψ^{non} by setting

$$\psi^{non}_{j,k,m}(x) = 2^{\frac{3}{4}j}\psi^{non}\left(S_k A_{2^j} x - M_{c_j} m\right) \tag{3}$$

where A_{2^j} is parabolic scaling matrix, S_k is shear matrix, and M_{c_j} is a sampling matrix given by $M_{c_j} = \text{diag}(c_1^j, c_2^j)$. We only discuss the case of the shearlet coefficients associated with A_{2^j} and S_k; the

same procedure can be applied to compute the shearlet coefficients associated with $\widetilde{A}_{2j}$ and $\widetilde{S}_k$. After faithfully digitizing $\psi^{non}_{j,k,m}$, the digital formulation of the discrete nonseparable shearlet transform (DNST) is given by

$$DNST_{j,k,m}\left(f_J\right)= \left(f_J * \overline{\psi}^d_{j,k}\right)\left(2^J A^{-1}_{2^j} M_{c_j} m\right) \text{ for } j = 0, \ldots, J-1 \tag{4}$$

where f_J is the scaling coefficients. $\psi^d_{j,k}$ is digital shearlet filters, $\psi^d_{j,k} = S^d_{k2^{-j/2}}\left(p_j * W_j\right)$, $S^d_{k2^{-j/2}}$ is the discrete shear operator, p_j is the Fourier coefficients of P, and $W_j = g_{J-j} \otimes h_{-j/2}$, g_{J-j} and $h_{J-j/2}$ are 1D filters. Please refer to reference [13] for details.

The frequency tiling induced by such discrete shearlet system is shown in Figure 2a, where $\hat{\phi}$, $\hat{\psi}^{non}$ and $\widetilde{\psi}^{non}$ are associated with the square in the center, the horizontal cone (white), and the vertical cone (yellow), respectively. Each scale corresponds to a ring of tiles and shear is associated with a pair of tiles in a certain direction within the ring. With a proper choice of the parameters associated with the translation, the DNST is obtained as a series of filtering operations. Each shearlet function has two symmetric tiles. The magnitude of the shearlet filter is shown in Figure 2b,c. Figure 2b is the frequency tiles of a DNST filter corresponding to the first scale. Figure 2c is the frequency tiles of a DNST filter corresponding to the second scale.
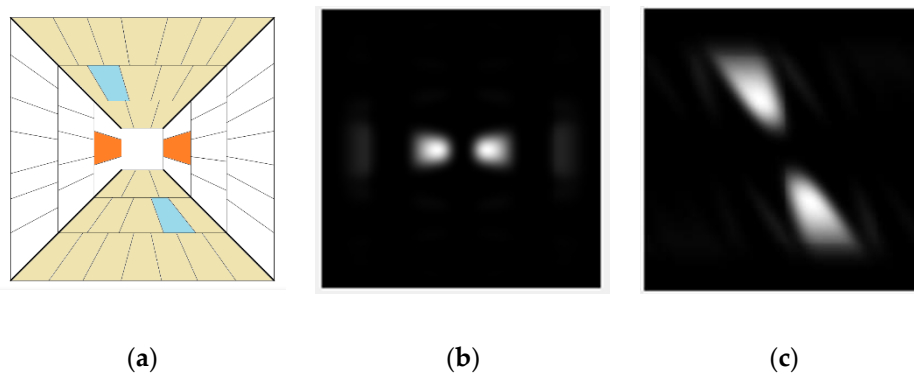

(a)   (b)   (c)

Figure 2. (**a**) The tiling of the ideal frequency plane by a cone adapted shearlet system. (**b**) The frequency tiles of a discrete nonseparable shearlet transform (DNST) filter corresponding to the first scale. (**c**) The frequency tiles of a DNST filter corresponding to the second scale.

3.2. Gray-Level Co-Occurrence Matrix

Gray-level co-occurrence matrix (GLCM) is an effective texture feature extraction approach. GLCM considers not only the distribution of intensities but also the relative positions of pixels in an image [25]. Let Q be an operator that defines the position of two pixels relative to each other, and consider an image, I_f, with possible intensity levels. Let G be a matrix whose element is the number of times that pixel pairs with intensities z_v and z_h occur in I_f in the position specified by Q. A matrix formed in this manner is referred to as a gray-level co-occurrence matrix. Generally, GLCM is not directly regarded as a texture feature, but it is represented by some descriptors such as energy, contrast, entropy, homogeneity, and correlation.

3.3. Kernel Spectral Regression

Kernel spectral regression (KSR) is a dimensionality reduction method based on manifold learning and subspace [18]. The KSR assumes that the original data is embedded in the low-dimensional manifold of the high-dimensional observation space, and each sample is kept adjacent to it by the manifold learning algorithm, so as to mine the low-dimensional manifold structure contained in the high-dimensional data. KSR only needs to solve a set of regularized least squares problems, which results in huge savings of both time and memory. KSR can make efficient use of label and local

neighborhood information to discover the intrinsic discriminant structure in the data. The algorithmic procedure is stated below.

(1) Constructing the adjacency graph. Let G denote a graph with m nodes. The *i-th* node corresponds to the sample x_i. If x_i shares the same label with x_j, put an edge between nodes i and j.

(2) Choosing the weights:

$$w_{ij} = \begin{cases} \frac{1}{l_k}, & if\ x_i\ and\ x_j\ both\ belong\ to\ the\ k-th\ class \\ 0 & otherwise \end{cases} \tag{5}$$

where W_{ij} is the weight of the edge joining vertices i and j.

(3) Responses generation. Find $y_0, y_1, \cdots, y_{c-1}$, the largest c generalized eigenvectors of eigenproblem.

$$W\mathbf{y} = \lambda D\mathbf{y} \tag{6}$$

where D is a diagonal matrix whose (i, i)-*th* element equals to the sum of the *i-th* column of W, c is the number of classes.

(4) Regularized kernel least squares. Find $c - 1$ vectors $\alpha_{1,\cdots}, \alpha_{c-1} \in R^m$. $\alpha_k(k = 1, \cdots c - 1)$ is the solution the linear equations system.

$$(K + \alpha I)\alpha_k = \mathbf{y}_k \tag{7}$$

where $K_{ij} = K(x_i, x_j)$. It can be easily verified that function $f(x) = \sum\limits_{i=1}^{m} \alpha_i^k K(x, x_i)$ is the solution of the following regularized kernel least square problem:

$$\min_{f \in H_K} \sum_{i=1}^{m} \left(f(x_i) - y_i^k\right)^2 + \alpha \| f \|_k^2 \tag{8}$$

(5) KSR Embedding: Let $\Theta = [\alpha_1, \alpha_2, \cdots, \alpha_{c-1}]$, Θ is a $m \times (c - 1)$ transformation matrix. The samples can be embedded into c − 1 dimensional subspace by

$$x \to z = \Theta^T K(:, x) \tag{9}$$

where $K(:, x) = [K(x_1, x), K(x_2, x), \cdots, K(x_m, x)]^T$.

4. Defect Recognition Algorithm

The defect recognition algorithm is the core of the surface quality inspection system. Generally, defect recognition algorithm consists of image preprocessing, image feature extraction, and image classification. In order to obtain more comprehensive information of the surface images of continuous casting slabs, we do not carry out image preprocess. Figure 3 is the schematic diagram of the defect recognition algorithm. The details are as follows.

(1) Extract DNST features. All sample images are decomposed into multiple subbands at different scales and different directions by DNST, and the coefficients matrices of subbands of horizontal and vertical cones are obtained. Then calculate the mean and variance statistics of each subband for all samples. The mean reflects the average value of the subband coefficient matrix, and the variance reflects the deviation between the subband coefficient and the average value of the subband coefficients. The DNST feature of each sample image is a one-dimensional long vector.

(2) Extract texture features. The gray level of the original image is compressed to reduce the computational complexity. The directions choose $0°$, $45°$, $90°$, and $135°$. The texture descriptors energy, contrast, entropy, homogeneity, and correlation are calculated for four directions,

respectively. Then, the mean and variance of each texture descriptor are calculated. Thus, each sample image can get a 10-dimensional GLCM texture feature vector.

(3) Feature combination. The DNST and GLCM feature vector of each sample are spliced into a new one-dimensional long vector. Then the feature vector of each sample are arranged from top to bottom to form the feature matrix. Finally, the feature matrix is normalized to [−1, 1].

(4) Dimensionality reduction. Since the extracted features are high-dimensional and redundant, which is not conducive to subsequent classification. Therefore, we first use the KSR to reduce the dimensionality of the feature matrix of the training set and use the projection matrix obtained from the training set to reduce the dimensionality of the feature matrix of the test set. The high-dimensional feature matrix reduced to c − 1 dimensional subspace, where c is the number of classes.

(5) Defect classification. First, the low-dimensional feature matrix is normalized to [−1, 1]. Then, the low dimensional features and labels data are input into the SVM [26] for training and classification. Finally, the surface defects of the continuous casting slabs are recognized.
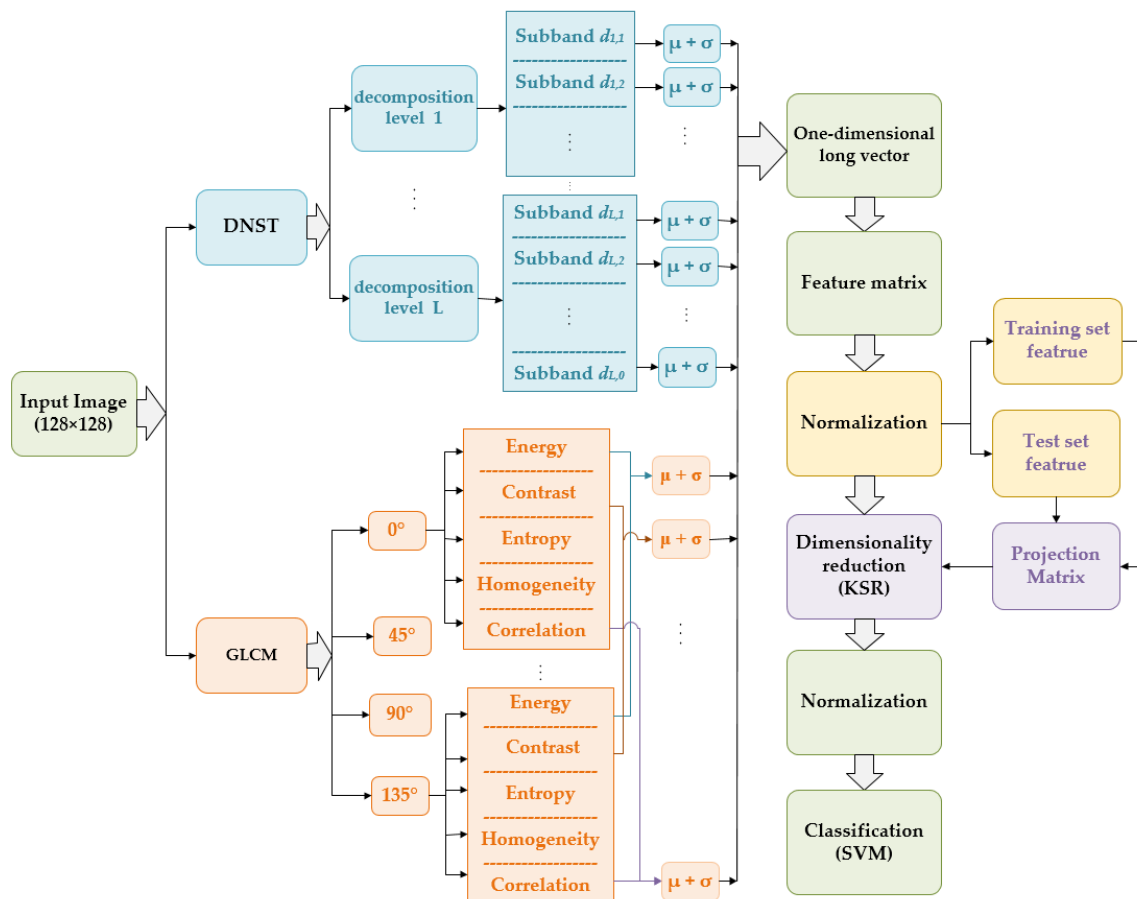

Figure 3. Schematic diagram of defect recognition algorithm.

5. Experiments and Discussions

In this section, the authors introduce the sample database in the experiment in Section 5.1. Some important parameters settings are explained in Section 5.2. In Section 5.3, the feature extraction results of DNST are presented and compared with three commonly used multi-scale methods and one texture extraction method. In Section 5.4, the experimental results of the proposed scheme are presented and compared with other feature combination schemes. The advantages of our proposed

scheme in classification time and accuracy are discussed in detail in Section 5.5. Finally, we analyze the specific classification and visualization results of the proposed schemes.

5.1. Sample Database

The samples were collected by an online surface inspection system on a continuous casting slabs production line in a steel plant. The defects database consists of 496 samples, which are divided into two types—positive samples and negative samples. The positive samples have crack defects, with 222 samples. The negative samples include three types of images—scales, lighting variations, and slag marks, with 274 samples. The cracks are defects, and the other three types of samples are pseudo-defects. The pseudo-defects are the main factor of false classification, so the pseudo-defects are labeled as a type of samples. The odd numbers of samples were used for the training set, and the even numbers of samples were used for the test set. All sample images are cropped to 128 by 128 pixels for classification.

5.2. Parameter Setting

To test the feature extraction performance of the proposed scheme, the proposed scheme is compared with wavelet, Contourlet, DST, GLCM, etc. Some important parameters are listed as follows.

DNST: The parameters chose [1 2], [0 1 2], etc. Take an example to explain parameters. When the parameter is set to [1 2], the first scale has eight shearlet direction filters, and the second scale has 16 direction filters, which produced a total of 24 high-frequency subbands and one low frequency subband. The number of DNST features is $(8 + 16 + 1) \times 2 = 50$.

GLCM: The gray level of the original image was compressed to 8, 16, 24 levels, etc. The distance parameter was set to 1.

Wavelet: The wavelet type chose "Haar," "db2," etc. The decomposition level was set to 2,3,4.

Contourlet: The Laplacian filter chose "9-7," and the directional filter chose "pkva." The direction parameter chose [2 3 4], [3 4 5], etc.

DST: The scale filter chose "Symmlet" with the fourth-order vanishing moment, scale parameter was set to [2 1 1], [2 1 1 0], etc. The directional parameters were set to [2 2 2], [2 2 3 3], etc.

KSR: The kernel type chose "Gaussian," and the kernel parameter was set to 0.001.

We chose the radial basis kernel (RBF) as the kernel function of the SVM classifier, and the kernel parameter gamma γ was set to iterate through all values from 0 to 4 with step length 0.01. The other parameters took the default values. Our experiments were based on using a ThinkPad E440 PC equipped with a 2.29 GHz Intel i7 processor and 8GB of RAM. The application software is MATLAB published by MathWork company.

5.3. Comparison of DNST Feature

Numerous experiments on each method were carried out and took the best value and average value as the objective basis of the comparison. The experimental results are shown in Figure 4. From Figure 4, the DNST feature achieves the highest classification results. The best accuracy is 89.92%, and the average accuracy is 89.36%. The Contourlet and DST schemes obtained the same recognition result. The average accuracy of DNST is 1.34% higher than that of DST and Contourlet, 3.15% higher than that of wavelet, and 5.97% higher than that of GLCM. This is due to the fact that DNST has excellent spatial localization properties and directional selectivity, and it can capture defects features more accurately for continuous casting slabs. The classification accuracy obtained by GLCM is the lowest, which indicates that only extracting texture information is not sufficient to represent features of the continuous casting slabs. Figure 4 also shows that the four multi-scale multi-directional feature extraction methods are superior to GLCM. Besides, the difference between the best accuracy and the average accuracy of the wavelet is $88.31\% - 86.21\% = 2.1\%$, which indicates that the wavelet is less robust to parameter changes. The difference between the best accuracy and average accuracy of DNST

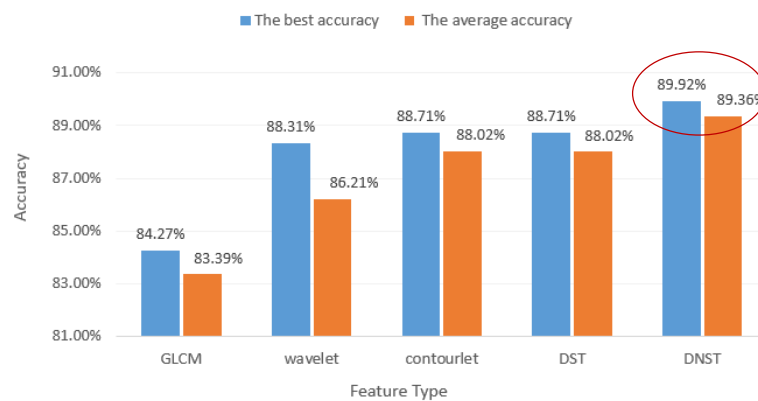is 89.92% − 89.36% = 0.56%, the value is lowest, which shows the DNST has better robustness for parameter changes.

Figure 4. Classification results of different features.

5.4. Comparison of Feature Combination

In addition to the classification accuracy evaluation metrics, the other commonly used evaluation metrics include recall, false positive rate (FPR), F-measurement, precision, the area under the receiver operating characteristic (ROC) curve (AUC), etc. [27]. The lower value of the FPR metrics indicates the better feature extraction performance, while the higher value of the other metrics indicates the better feature extraction performance.

In order to verify the superiority of the proposed scheme DNST-GLCM-KSR, we compared it with the Contourlet-KLPP scheme in reference [1], the DST-KLPP scheme in reference [2], Contourlet-GLCM-KLPP in reference [11], as well as with several similar combination feature schemes. Table 1 lists classification results of some evaluation metrics. From Table 1, the DNST-GLCM-KSR scheme achieves the lowest value of FPR, the highest values of precision, F-measure, AUC, and accuracy, indicating that the proposed scheme obtained the best comprehensive performance in the seven schemes. Besides, when only extracting DNST features, using the KLPP algorithm to reduce dimension can achieve better metrics than that of using KSR except AUC metrics. When extracting DNST-GLCM features, using KSR algorithm to reduce dimension can achieve better metrics than that of using KLPP. The above shows that both dimensionality reduction technologies are effective, and which one is better to use depends on experiments. The principle of the two technologies is the same, but the calculation technic is different.

Table 1. Results of different evaluation metrics.

Feature	FPR (%)	Precision (%)	F-Measure (%)	AUC	Accuracy (%)
Contourlet-KLPP	6.57	92.04	92.79	0.961	93.55
Contourlet-GLCM-KLPP	5.11	93.69	94.09	0.967	94.35
DST-KLPP	5.11	93.69	94.09	0.972	94.35
DNST-KSR	6.57	92.17	93.25	**0.976**	94.35
DNST-KLPP	5.84	93.04	94.09	**0.973**	95.16
DNST-GLCM-KLPP	3.65	95.41	95.15	0.979	95.16
DNST-GLCM-KSR	**2.92**	**96.36**	**96.37**	**0.980**	**96.37**

Taking the accuracy metrics as an example, DNST-GLCM-KSR scheme achieved the highest accuracy of 96.37%, which is 2.82% higher than that of reference [1] and 2.02% higher than that of [2] and [11], indicating that the proposed scheme is superior to the traditional ones. When using the same dimensionality reduction technology, the accuracy of Contourlet-KLPP is 93.55%, DST-KLPP is 94.35%, and DNST-KLPP is 95.16%, which indicates that the DNST can extract more discriminant

features of continuous casting slabs than that of Contourlet and DST. The above results show that DNST-GLCM-KSR is an excellent feature fusion approach for continuous casting slabs.

5.5. Comparisons of Dimensionality Reduction

Table 2 lists the results of different combined features of DNST. It can be seen that the accuracy of the training set and the test set of DNST-GLCM is 96.77% and 90.73% respectively, the accuracy of the training set and the test set of DNST is 93.55% and 89.92% respectively, and both results of DNST-GLCM are higher than those of DNST, which indicates DNST feature combined with GLCM texture features can improve the recognition accuracy. In addition, the accuracy of DNST-KSR is $94.35\% - 89.92\% = 4.43\%$ higher than that of DNST, and the accuracy of DNST-GLCM-KSR is $96.37\% - 90.73\% = 5.64\%$ higher than that of DNST-GLCM. The above shows that KSR can effectively remove redundancy and interference features and improve recognition accuracy. At the same time, we noticed that the classification time was shortened from tens of seconds to several seconds by KSR. This is because KSR reduces feature dimensionality to $c - 1$, where c is the number of classes. The continuous casting slabs samples include positive samples and negative samples—that is to say, the number of classes is 2. The feature number was reduced to 1 dimensionality. Finally, it should be noted that the number of subbands by DNST decomposition is different when different feature combinations achieve the highest recognition accuracy.

Table 2. Result of feature combination.

Feature Type	The Number of Features	Time Cost (ms)	Accuracy (%)	
		Classification	Training Set	Test Set
DNST	66	33.10	**93.55**	89.92
DNST-GLCM	36	25.04	**96.77**	90.73
DNST-KSR	1	3.39	96.37	94.35
DNST-GLCM-KSR	**1**	**3.13**	97.58	**96.37**

Figure 5 shows the recognition accuracy of the training set and test set when using KSR and not using KSR. With the increase of SVM kernel parameter γ, the accuracy of the DNST-GLCM training set gradually increases and is finally close to 100%, while the accuracy of the test set first increases and then decreases, which indicates that DNST-GLCM feature data is sensitive to SVM kernel parameter; in other words, the feature is complex and not conducive to classifier learning. For DNST-GLCM-KSR, the accuracy of test set and training set are both high, and the curve fluctuation are small. The above results show that the DNST-GLCM-KSR scheme makes the extracted features more discriminative, easier to learn and classify, and it has a strong robustness to the kernel parameter of SVM.
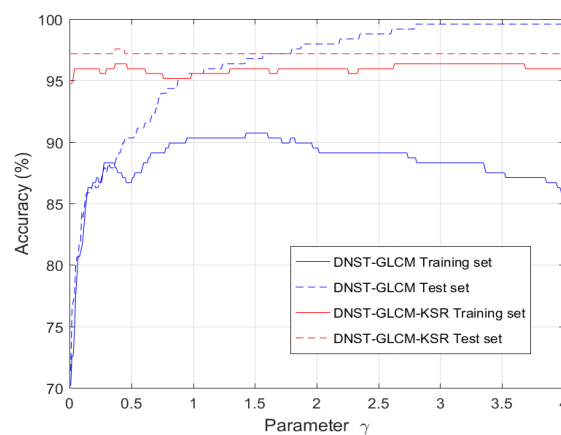

Figure 5. The recognition accuracy of training set and test set.

5.6. Confusion Matrix and Visualization

Table 3 lists the detailed classification of test set of DNST-GLCM-KSR scheme. The accuracy of positive sample (crack defect) is 95.50%; the accuracy of negative sample is 97.08%. There are four pseudo-defects misclassified as crack defects, and five crack defects are misclassified as pseudo-defects. This was due to the fact that inter-class defects have similar aspects in appearance. The false alarm rate of cracks is 4/110 = 3.64%, and the missing alarm rate is 5/111 = 4.5%. The above metrics meet the needs of engineering application of continuous casting slabs.

Table 3. The confusion matrix of discrete nonseparable shearlet transform gray-level co-occurrence matrix kernel spectral regression (DNST-GLCM-KSR) scheme.

Sample Type	Positive Sample	Negative Sample	Correct Number	Sample Total	Accuracy
Positive sample	106	**5**	106	111	95.50%
Negative sample	**4**	133	133	137	97.08%
total	110	138	239	248	96.37%

Figure 6 shows the visualization of the DNST-GLCM-KSR test set. The result is a straight line, because the number of the feature dimensionality is 1. The pink circle represents the positive sample, the blue one represents the negative sample, and the upper left corner is a local enlargement image. The result of Figure 6 is consistent with that of Table 3, namely that four pseudo-defects are misclassified as crack and five crack defects are misclassified as pseudo-defects. From the graph, we can see that the DNST-GLCM-KSR features truly reflect the similarity between defect images. The intra-class scatter is small, and the inter-class scatter is large. The above analysis shows the method proposed can effectively recognize crack defects of continuous casting slabs in complex background images and interference factors.
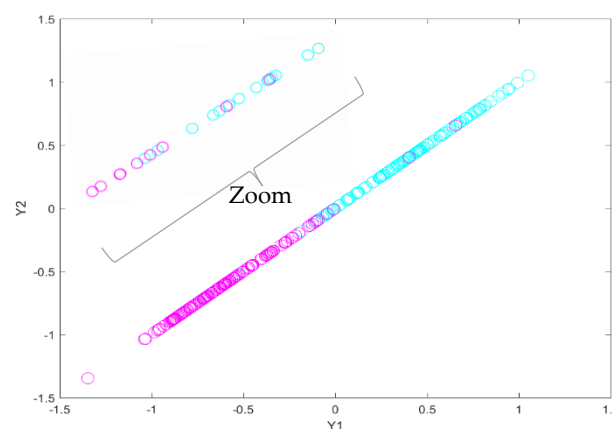

Figure 6. Visualization results.

6. Conclusions

According to the direction and texture information of surface defects of the continuous casting slabs with complex backgrounds, a new feature extraction approach DNST-GLCM-KSR is proposed, which combines multi-scale and multi-directional DNST features with GLCM texture features and uses KSR technology to reduce dimensionality. The experimental results are as follows.

(1)　The DNST feature obtained the highest average accuracy and the best accuracy. It can better characterize defects of continuous casting slabs than that of Contourlet, DST, wavelet, and GLCM.

(2)   The accuracy of the training set and test set of the DNST-GLCM feature were 96.77% and 90.73%, respectively. Both results were higher than those of DNST feature. The recognition accuracy of continuous casting slabs can be improved by combining the features of DNST and GLCM.

(3)   The recognition accuracy of the DNST-GLCM-KSR scheme is 5.64% higher than that of DNST-GLCM, and the classification time of DNST-GLCM-KSR was shorter than that of DNST-GLCM. Using KSR technology can improve recognition accuracy and shorten classification time.

(4)   The proposed scheme can extract more discriminative features of defects and make the recognition accuracy of crack defect up to 95.50% and the total accuracy up to 96.37%. The new scheme provides a new method for the surface defect recognition of continuous casting slabs.

(5)   Future work should collect more defect samples, establish a complete sample database, and improve the recognition accuracy of crack defect.

References

1.   Ai, Y.; Xu, K. Feature extraction based on contourlet transform and its application to surface inspection of metals. *Opt. Eng.* **2012**, *51*, 113605. [CrossRef]

2.   Xu, K.; Liu, S.; Ai, Y. Application of shearlet transform to classification of surface defects for metals. *Image Vis. Comput.* **2015**, *35*, 23–30. [CrossRef]

3.   Wei, S.; Zheng, S.; Gong, H.; Tang, H. Study on On-line Detection of the Cast-billet Surface Defect. *J. Wuhan Univ. Technol. (Inf. Manag. Eng.)* **2009**, *31*, 433–436.

4.   Cai, K.; Sun, Y.; Han, C. The "Zero Defect" Philosophy of Controlling Strand Quality for Steel Continuous Casting. *Contin. Cast.* **2011**, *s1*, 288–298.

5.   Zhang, Y.; Cheng, W.S.; Zhao, J. Classification of surface defects of strips based on invariable moment functions. *Opt. Electron. Eng.* **2008**, *35*, 90.

6.   Xu, K.; Yang, C.L.; Zhou, P. Technology of on-line surface inspection for hot-rolled steel strips and its industrial application. *J. Mech. Eng.* **2009**, *45*, 111. [CrossRef]

7.   Song, K.; Yan, Y. A noise robust method based on completed local binary patterns for hot-rolled steel strip surface defects. *Appl. Surf. Sci.* **2013**, *285*, 858–864. [CrossRef]

8.   Ban, J.; Seo, M.; Goh, T.; Jeong, H.; Kim, S.W.; Koo, G.; Shin, C.; Choi, H.; Lee, J.-H.; Kim, S.W.; et al. Automatic detection of cracks in raw steel block using Gabor filter optimized by univariate dynamic encoding algorithm for searches (uDEAS). *NDT E Int.* **2009**, *42*, 389.

9.   Pan, E.; Ye, L.; Shi, J.; Chang, T.-S. On-line bleeds detection in continuous casting processes using engineering-driven rule-based algorithm. *J. Manuf. Sci. Eng.* **2009**, *131*, 061008. [CrossRef]

10.   Xu, K.; Yang, C.L.; Zhou, P.; Yang, C. On-line detection technique of surface cracks for continuous casting slabs based on linear lasers. *J. Univ. Sci. Technol. Beijing* **2009**, *31*, 1620.

11.   Ke, X.U.; Yang, C.L.; Peng, Z.; Yang, C. Recognition of surface deffects in continuous casting slabs based on Contourlet transform. *J. Univ. Sci. Technol. Beijing* **2013**, *35*, 1195–1200.

12.   Tian, S.-Y.; Xu, K.; Guo, H.-Z. Application of local binary patterns to surface defect recognition of continuous casting slabs. *Chin. J. Eng.* **2016**. [CrossRef]

13.   Lim, W.-Q. Nonseparable shearlet transform. *IEEE Trans. Image Process.* **2013**, *22*, 2056–2065. [PubMed]

14.   Kutyniok, G.; Lim, W.Q.; Reisenhofer, R. ShearLab 3D: Faithful Digital Shearlet Transforms based on Compactly Supported Shearlets. *arXiv* **2014**, arXiv:1402.5670. [CrossRef]

15.   Kang, R.; Cao, B.; Wang, B.; Yan, L.; Qu, G. Compressed sensing longitudinal MRI based on wavelet and shearlet. *J. Beijing Jiaotong Univ.* **2017**, *41*, 127–132.

16. Pejoski, S.; Kafedziski, V.; Gleich, D. Compressed Sensing MRI Using Discrete Nonseparable Shearlet Transform and FISTA. *IEEE Signal Process. Lett.* **2015**, *22*, 1566–1570. [CrossRef]

17. Liu, L.; Kuang, G.Y. Overview of image textural feature extraction methods. *J. Image Graph.* **2009**, *4*, 622–635.

18. Cai, D.; He, X.; Han, J. *Spectral Regression for Dimensionality Reduction*; Technical Report; UIUC: Champaign, IL, USA, 2007.

19. Cai, D. Spectral Regression: A Regression Framework for Efficient Regularized Subspace Learning. Ph.D. Thesis, UIUC, Champaign, IL, USA, 2009.

20. Donoho, D.L. Orthonormal ridgelets and linear singularities. *Siam J. Math. Anal.* **2000**, *31*, 1062–1099. [CrossRef]

21. Candes, E.; Demanet, L.; Donoho, D.; Ying, L. Fast discrete Curvelet transforms. *Multiscale Model. Simul.* **2006**, *5*, 861. [CrossRef]

22. Po, D.; Do, M. Directional multiscale modeling of images using the contourlet transform. *IEEE Trans. Image Process.* **2006**, *15*, 1620. [CrossRef]

23. Lim, W.Q. The discrete shearlet transform: A new directional transform and compactly supported shearlet frames. *IEEE Trans. Image Process.* **2010**, *19*, 1166–1180. [PubMed]

24. Pennec, E.L.; Mallat, S. Sparse geometric image representations with bandelets. *IEEE Trans. Image Process.* **2005**, *14*, 423–438. [CrossRef] [PubMed]

25. Gonzalez, R.C.; Woods, R.E. *Digital Image Processing*, 3rd ed.; Prentice-Hall, Inc.: Upper Saddle River, NJ, USA, 2007.

26. Chang, C.C.; Lin, C.J. LIBSVM: A library for support vector machines. *ACM Trans. Intell. Syst. Technol.* **2011**, *2*, 1–27. [CrossRef]

27. Zhou, Z. *Machine Learning*; Tsinghua University Press: Beijing, China, 2016.